Molecular treatment of electron capture by protons from the ground and excited states of alkali-metal atoms

M. Kimura and R. E. Olson
Physics Department, University of Missouri-Rolla, Rolla, Missouri 65401

J. Pascale
Service de Physique des Atomes et des Surfaces, Centre d'Etudes Nucléaires de Saclay, 91191 Gif-sur-Yvette Cedex, France

(Received 24 June 1982)

Electron-capture cross sections for H^+ plus alkali-metal atom (Na, K, Rb, and Cs) systems have been computed for projectile energies from 10 eV to 10 keV. An impact-parameter perturbed-stationary-state theory using molecular states that incorporate electron translation factors was used to calculate the cross sections. The wave functions were generated by employing the pseudopotential method. These yield equilibrium parameters R_e and D_e for the $A\,^2\Sigma^+$ molecular state that are in good agreement with *ab initio* results. Interaction energies are also presented for the LiH^+ system. Basis sets of up to eight molecular states were used to calculate the electron-capture cross sections from ground (ns) as well as from the first excited (np) states of the alkali-metal atoms. Results for electron capture from the ground-state alkali-metal atom are in good agreement with the recent experiments of Nagata. Electron capture from excited alkali-metal (np) atoms does not yield enhanced cross sections relative to capture from the ground state and, in fact, shows decreased cross sections for the heavy alkali-metal atoms. Such behavior is contrary to predictions made using arguments based on the magnitude of the energy gap ΔE to the electron-capture product states.

I. INTRODUCTION

Recently, processes of electron capture by protons on alkali-metal (M) atoms have been of both theoretical[1–6] and experimental interest.[7–11] Much of this interest is motivated by the use of alkali-metal atom targets in polarized-atom and negative-ion beam sources. Experimentally, with the use of a laser, it has now become possible to pump the first excited state of the alkali-metal atoms and measure the electron-capture cross sections for collisions with protons.

In this paper we address the problem of electron capture from the ground electronic state as well as from the first excited electronic state and present calculated cross sections for

$$H^+ + M(ns) \rightarrow H + M^+ \quad (1)$$

and

$$H^+ + M^*(np) \rightarrow H + M^+ , \quad (2)$$

where n is the alkali-metal–atom valence-electron principal quantum number ($n=3$ for Na to $n=6$ for Cs). The collision-energy range investigated was from 10 eV to 10 keV with $M \equiv$ Na, K, Rb, and Cs. Detailed cross sections for production of H($1s$), H($2s$), and H($2p$) are also given and the cross sections are compared to recent experimental data.

A recent interesting measurement is one achieved by Kushawaha *et al.*[10] for electron capture in the $H^+ + Na(3s)$ and $H^+ + Na^*(3p)$ systems at collision energies from 5 eV to 1 keV. These authors observed that the ratio of the Lyman-α production cross sections for $H^+ + Na^*(3p)$ and $H^+ + Na(3s)$ collisions is nearly unity for $E \geq 10$ eV. These observations have not been justified theoretically. One of our goals was to understand these experiments and predict results for similar types of measurements on the heavier alkali-metal atom systems.

Most of the theoretical effort has been concentrated on the $H^+ + Cs$ system in the energy region $E \approx 0.1 \sim 10$ keV, since this system provides insight into electron-capture mechanisms between near-

resonant initial and final channels.[1-5] The theoretical calculations that determine electron-capture cross sections for the $H^+ + Cs$ system are based upon a molecular treatment with the use of the perturbed-stationary-state (PSS) method.[12] The results are usually in good agreement with those of experiment.

More recently, Kubach and Sidis[6] have performed a series of calculations for electron capture in $H^+ + M$ collisions using a molecular-state expansion basis generated by the projected-valence-bond (PVB) method. For the $H^+ + K$ and $H^+ + Rb$ systems their results agree well with recent measurements in the energy range of 0.1 to 6 keV. For the $H^+ + Na$ system, however, the results were in marked disagreement with the measurements, particularly at collision energies below ~ 2 keV. Their reasoning for the discrepancy is attributed to experimental error, because good agreement was obtained for the $H^+ + K$ and $H^+ + Rb$ systems. Since Kubach and Sidis[6] did not provide detailed information about their calculation in the paper, one cannot definitively determine the origin of the discrepancies. However, their method for generating molecular eigenstates and eigenvalues adopted an exceedingly small Slater-type-orbital (STO) basis in the PVB expansion which displayed incorrect asymptotic energies. Because the dynamical coupling terms are very sensitive to the quality of the wave functions, any inaccuracy in them can lead to serious error in the cross-section evaluation.

In this study we have employed a molecular-state expansion basis set with associated molecular electron translation factors (ETF's) based on a formulation derived from the time-dependent Schrödinger equation.[13] Only recently, the important effects of ETF's in calculations of slow ion-atom collisions have been noticed. Some limited studies[13-16] about the effects have clearly indicated that the neglect of the ETF's causes spurious long-range couplings and in some cases yields completely unphysical results. Therefore, the inclusion of ETF's within the framework of a molecular treatment is indispensable. An excellent review article about the subject can be found in Ref. 17.

Our studies on the $H^+ + M$ systems focus on the following: (i) the generation of molecular eigenstates by the use of the pseudopotential method,[18] (ii) the inclusion of ETF effects to evaluate the nonadiabatic couplings, and (iii) the determination of the total and detailed electron-capture cross sections from both the ground and the first excited state of the alkali-metal atoms in the collision-energy regime of 10 eV to 10 keV.

II. THEORETICAL METHOD

A. Molecular states

One method used to generate the molecular eigenstates of the $[H+M]^+$ systems is to solve the Schrödinger equation with the full electronic Hamiltonian. This method is very cumbersome as well as time consuming, especially for the heavier alkali-metal atoms. To remove some of these difficulties a pseudopotential is used to replace the potential produced by the core electrons and nucleus of the alkali-metal atom. This reduces the calculation to a much simpler one-electron problem. Since the details of the technqiue are well established and various articles about the subject have been published, we will not repeat them here and refer the interested reader to the review by Bardsley.[18]

Therefore, it is sufficient to summarize some features of this method. The one-electron Schrödinger equation which represents the wave function of a valence electron in the molecular ion $[H+M]^+$ is given by

$$\left[-\frac{1}{2}\nabla_r^2 + V_A(\vec{r}_A) - \frac{1}{r_B} + \frac{1}{R} - E_i(R)\right]\Psi_i(\vec{r},R) = 0 , \quad (3)$$

where $\vec{r}_A$ and $\vec{r}_B$ are the position vectors of the valence electron with respect to the alkali-metal ion core and the H^+ nucleus, respectively. The eigenvalue $E_i(R)$ and eigenfunction $\Psi_i(\vec{r},R)$ depend parametrically on the internuclear coordinate R (Born-Oppenheimer approximation) and $V_A(\vec{r}_A)$ represents the interaction between the valence electron and the alkali-metal ion core. This term is replaced by a pseudopotential. The pseudopotential we chose is an l-dependent Gaussian type of the form

$$V(\vec{r}) = \sum_{l,m} V_l(r) \mid Y_{lm} \rangle \langle Y_{lm} \mid \quad (4a)$$

with

$$V_l(r) = A_l \exp(-\xi_l r^2) - \frac{\alpha_d}{2(r^2+d^2)^2} - \frac{\alpha_q}{2(r^2+d^2)^3} - \frac{1}{r} , \quad (4b)$$

where $\mid Y_{lm} \rangle$ are the spherical harmonics. The parameters A_l, ξ_l, α_d, α_q, and d have been chosen to fit spectroscopic data and are tabulated by Bardsley.[18]

The electronic wave function $\Psi(\vec{r},R)$ is con-

structed using a two-center expansion in terms of a linear combination of atomic orbitals—molecular orbital treatment (LCAO-MO). Fixed orbital exponents in a STO basis are employed. The form of $\Psi(\vec{r},R)$ is given in terms of STO orbitals,

$$\Psi(\vec{r},R)=\sum_i c_i\chi_i^{\mathrm{STO}}(\vec{r}_A)+\sum_j d_j\chi_j^{\mathrm{STO}}(\vec{r}_B)\ . \tag{5}$$

For the $^2\Sigma^+$ molecular states 18 STO's (9 STO's on each center) have been employed. The individual basis sets include p and d orbitals to account for polarization effects. For the $^2\Pi$ molecular states 16 STO's (8 STO's on each center) have been employed. The basis sets and the exponents used are tabulated in Table I. The alkali-metal atom $(n-1)s$-, ns-, and np-orbital exponents (where n represents the principal quantum number of the ground-state valence electron) are from Stevens *et al.*,[19] while the hydrogen-atom basis set is from the previous work of Olson *et al.*[20] For each alkali-metal atom two additional $3d$ orbitals and one $(n+1)s$ orbital were added and the exponents optimized for the lowest energy of the representative atomic level. With this basis set and the pseudopotentials of Bardsley[18] the atomic energies of the $H(1s)$ and $H(n=2)$ levels are exact, while the average error in the ionization energies of the four lowest electronic levels of the alkali-metal atoms is 0.0034 eV with the maximum deviation being 0.0081 eV.

Our calculated results for the equilibrium parameters R_e and D_e of the $A\,^2\Sigma^+$ state are presented in Table II and compared to other theoretical results. These pseudopotential calculations are in good agreement with the *ab initio* results[20] for NaH^+ and KH^+. As a test of our basis set we expanded the basis set to 29 STO's from 18 STO's and found only slight changes in the equilibrium parameters; the results are also given in Table II.

The calculated interaction energies for the $[H+M]^+$ systems are shown in Figs. 1 to 5. For the NaH^+ and KH^+ cases *ab initio* results[20] are also included and agree well with the present calculations. The general features of the potential curves are the following: (i) progressing from Li to Cs, the energy gap between the $A\,^2\Sigma^+$ and the $B\,^2\Sigma^+$ molecular states decreases causing the location of the avoided crossing between the $A\,^2\Sigma^+$ and $B\,^2\Sigma^+$ states to shift toward larger R ($\sim 11a_0$ for Na to $19a_0$ for Cs), (ii) the position of a narrowly avoided crossing between the $^2\Sigma^+$ states dissociating to the $H(n=2)$ manifold shifts outward ($R\sim 6a_0$ for NaH^+ to $R\sim 9a_0$ for CsH^+), even though the energy separation at the crossing point stays almost constant, (iii) the $B\,^2\Sigma^+$ and $C\,^2\Pi$ states of $H(n=2)+M^+$ cross at $8a_0$ for NaH^+ to $12a_0$ for CsH^+, so one can expect strong rotational coupling around this point. Also, the $C\,^2\Pi$ state approaches very closely to the $A\,^2\Sigma^+$ state for all systems at $R<5a_0$. Such behavior may influence the electron capture allowing strong rotational coupling between the $A\,^2\Sigma^+$ and $C\,^2\Pi$ states at small R. It should be noted that the pseudopotential method becomes invalid at $R\lesssim 2a_0$ where core-core overlap becomes significant. However, as far as the scattering is concerned, the important couplings occur at relatively large-R values ($R\gtrsim 5a_0$) and therefore, the calculated cross sections are relatively insensitive to the small-R region.

B. Coupled equations

We have assumed that the relative motion of the heavy particles is described by a classical trajectory.

TABLE I. Slater-orbital basis-set exponents.

	H	Li	Na	K	Rb	Cs
$(n-1)s$		0.412	0.790	1.135	1.473	1.620
ns	2.000	1.610	2.487	1.134	1.456	1.569
	1.000	0.732	0.694	0.689	0.831	0.903
	0.500	0.300	0.372	0.394	0.453	0.494
$(n+1)s$	0.500	0.375	0.290	0.352	0.348	0.302
	0.333					
np	1.000	2.013	0.721	0.820	1.063	1.200
	0.500	0.501	0.558	0.556	0.671	0.743
	0.333					
$3d$	0.333	0.701	1.484	1.770	1.290	1.149
		0.333	0.337	0.394	0.412	0.467

TABLE II. Equilibrium distance R_e (a.u.) and well depth D_e (eV) for the $A\,^2\Sigma^+$ states.

		Present[a]	Ref. 4	Ref. 20	Ref. 6	Ref. 8
LiH^+	R_e	7.47 (7.47)				
	D_e	0.47 (0.49)				
NaH^+	R_e	7.89 (7.87)	8.2	7.98±0.1	8.7	
	D_e	0.42 (0.46)	0.34	0.47±0.05	0.39	
KH^+	R_e	8.68 (8.58)	8.6	8.75±0.3	9.4	
	D_e	0.63 (0.68)	0.49	0.61±0.1	0.49	
RbH^+	R_e	8.87 (8.85)	8.8		10.4	
	D_e	0.68 (0.73)	0.50		0.55	
CsH^+	R_e	9.20 (9.17)	9.0		10.4	10 ±1
	D_e	0.82 (0.86)	0.70		0.71	0.77±0.05

[a]In the present results numbers shown without parentheses were obtained with the 18-term basis set given in Table I and used in the scattering calculations. The numbers in parentheses test the convergence of the calculations and are for a 29-term wave function with an expanded basis set which includes $(n+2)s$, $(n+1)p$, $4d$, and $4f$ optimized functions.

The total electronic wave function is expanded in the ETF modified Born-Oppenheimer (BO) wave function,

$$\Psi(\vec{r},t)=\sum_i a_i(t)\phi_i^{\mathrm{BO}}(\vec{r};\vec{R})F_i(\vec{r};R)\ , \tag{6}$$

where $\phi_i^{\mathrm{BO}}(\vec{r};\vec{R})$ is obtained from the pseudopotential calculations; it is the eigenfunction of the electronic Hamiltonian with eigenvalue $E_i(R)$ that depends parametrically on R. $F_i(\vec{r};R)$ includes electron translation factors of the form

$$F_i(\vec{r};R)=\exp\left[\left(\frac{im}{2\hbar}\right)f_i(\vec{r};R)\vec{r}\cdot\vec{V}\right]\ , \tag{7}$$

where $\vec{V}$ is the relative velocity of the heavy particles and $f_i(\vec{r};R)$ represents the switching function used[13,21] to incorporate the two-center molecular character into the ETF's. To obtain the coupled equations we substitute Eq. (6) into the time-dependent Schrödinger equation, multiply by

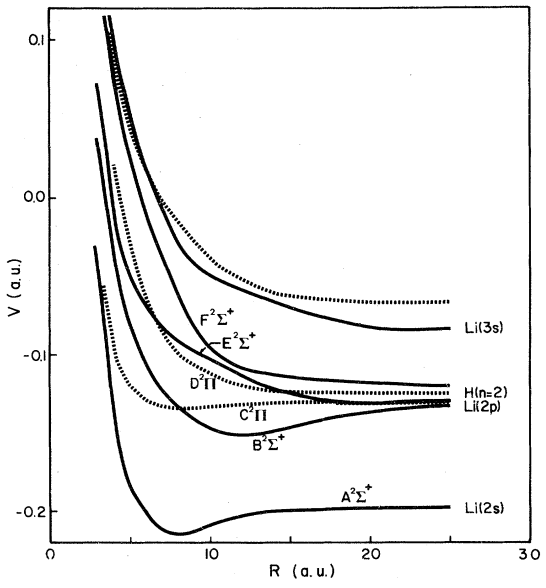

FIG. 1. Interaction energies calculated for the LiH^+ system. The $^2\Sigma^+$ molecular states are denoted by solid lines and the $^2\Pi$ states by dashed lines.

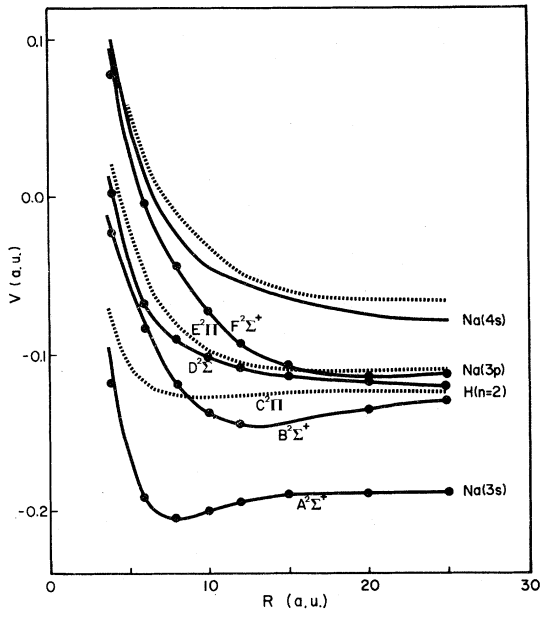

FIG. 2. Interaction energies for NaH^+. The notations are the same as in Fig. 1 and the circles are the results of *ab initio* calculations (Ref. 20) for the $A\,^2\Sigma^+$, $B\,^2\Sigma^+$, $D\,^2\Sigma^+$, and $F\,^2\Sigma^+$ states.

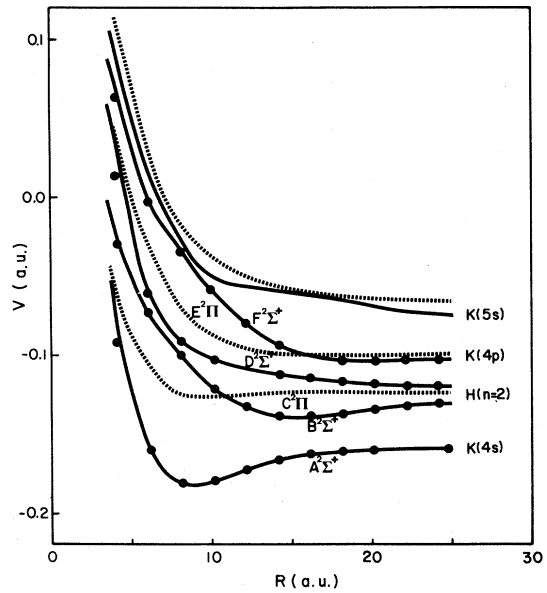

FIG. 3. Interaction energies for KH^+. The notations are the same as in Fig. 1 and the circles are the results of *ab initio* calculations (Ref. 20) for the $A\,^2\Sigma^+$, $B\,^2\Sigma^+$, $D\,^2\Sigma^+$, and $F\,^2\Sigma^+$ states.

$\phi_k^{*\mathrm{BO}} F_k^*$ from the left, integrate with respect to the electronic coordinates, expand the ETF's in powers of velocity $\vec{V}$, and retain the first-order terms of $\vec{V}$. This leads to the set of coupled equations

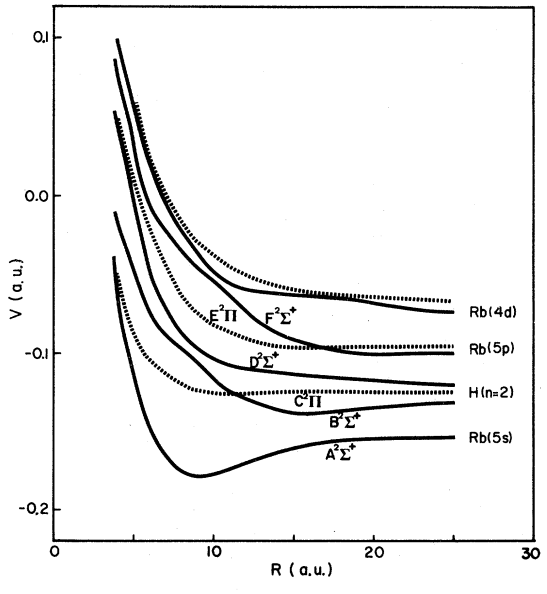

FIG. 4. Interaction energies for RbH^+. The notations are the same as in Fig. 1.

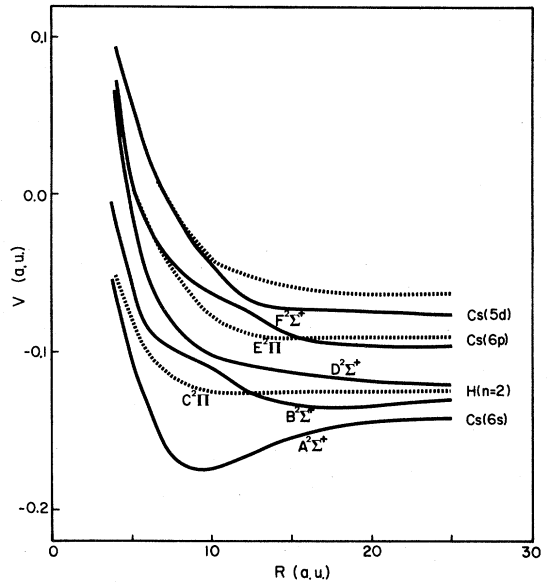

FIG. 5. Interaction energies for CsH^+. The notations are the same as in Fig. 1.

$$\dot{a}_j(t)=\sum_{i\neq j}\vec{V}\cdot(\vec{P}+\vec{A})a_i \times\exp\left[-\frac{i}{\hbar}\int^t[E_j(t')-E_i(t')]dt'\right]. \tag{8}$$

Here $\vec{P}$ and $\vec{A}$ are the nonadiabatic coupling and the correction terms due to the inclusion of ETF's, respectively. They have the form

$$\vec{P}_{ki}=\langle k\mid -i\hbar\vec{\nabla}_{\vec{R}}\mid i\rangle , \tag{9}$$

$$\vec{A}_{ki}=\langle k\mid[H_{\mathrm{el}},\vec{S}_i]\mid i\rangle =(E_k-E_i)\langle k\mid\vec{S}_i\mid i\rangle , \tag{10}$$

$$\vec{S}_i=\tfrac{1}{2}f_i(\vec{r};R)\vec{r} , \tag{11}$$

where the $\vec{V}\cdot(\vec{P}+\vec{A})$ terms can be divided into two contributions in the rotating-frame coordinate system

$$\vec{V}\cdot(\vec{P}+\vec{A})=\dot{R}(P^R+A^R)+\dot{\theta}(P^\theta+A^\theta) , \tag{12}$$

with

$$P_{ki}^R=\left\langle k\left|i\hbar\frac{\partial}{\partial R}\right|i\right\rangle , \qquad A_{ki}^R=(E_k-E_i)\langle k\mid\tfrac{1}{2}f_iz\mid i\rangle , \tag{13}$$

and

$$P_{ki}^{\theta}=\langle k \mid i\hat{L}_y \mid i \rangle \ , \tag{14}$$
$$A_{ki}^{\theta}=(E_k-E_i)\langle k \mid \tfrac{1}{2}f_i x \mid i \rangle \ .$$

The first term in Eq. (12) represents the radial coupling and the second term in Eq. (12) is the rotational (angular) coupling with its corresponding ETF correction term. $\dot{R}$ and $\dot{\theta}$ describe radial and angular velocities, respectively, and in the impact-parameter approximation, they can be written

$$\dot{R}=\frac{v_0 z}{R} \ , \ \dot{\theta}=\frac{bv_0}{R^2} \ , \tag{15}$$

where b is the impact parameter and v_0 is the relative velocity of the collision.

There has been a growing awareness about how to choose, or determine uniquely, the switching function to describe the two-center character properly and satisfy the boundary conditions in the molecular-state treatment.[21,22] Since we have employed the two-center LCAO-MO-STO wave function given in Eq. (5) as the molecular eigenstate, we can attach well-defined atomic ETF's to each basis function. This approach is sometimes called a "generalized traveling orbital method.[22,23] Our nonadiabatic coupling matrix elements are non-Hermitian, resulting from different switching functions for each state.

In the evaluation of the $(\vec{P}+\vec{A})$ matrix elements for the radial and rotational couplings we have used Gauss-Laguerre and Gauss-Legendre numerical integration and found that ten points are sufficient to maintain four to five significant-digit accuracy. The coupled equations were integrated numerically with the use of the method of Bulirsch and Stoer[24] with a relative truncation error automatically maintained between 10^{-4} and 10^{-5}.

The initial condition for solving the coupled equations is $a_k(-\infty)=\delta_{ik}$, if i designates the initial state. Therefore, the probability of finding the products in molecular state k is given by

$$P_k(E,b)=\mid a_k(+\infty;b) \mid^2 \ , \tag{16}$$

and the corresponding integrated cross section is

$$Q_k(E)=2\pi \int_0^{\infty} db \, bP_k(E,b) \ . \tag{17}$$

It can be shown[21] that Eq. (8) conserves unitarity for non-Hermitian coupling matrix elements with errors of order $(\vec{V})^2$ caused by the neglect of the second- and higher-order terms of $\vec{V}$ in Eq. (7). For most of the cases with $E \geq 0.1$ keV we used a linear trajectory (impact-parameter approximation) for its simplicity. However, in very slow collisions, $E \leq 0.1$ keV, the linear trajectory does not accurately describe the heavy-particle motion, since the deviation from the linear trajectory due to the repulsive wall of the potential is not negligible. Therefore, in this energy region, we have employed a screened Coulomb trajectory which corresponds to the repulsive wall of the incident channel.

III. RESULTS

A. Coupling

In Fig. 6 the long-range radial couplings from the $A\,^2\Sigma^+$ to the $B\,^2\Sigma^+$ states are displayed along with the potential difference $\Delta E(R)$. The $A\,^2\Sigma^+ \rightarrow B\,^2\Sigma^+$ coupling is very strong and dominates the electron-capture process in proton-alkali-metal atom collisions. The general trends of this coupling and the $\Delta E(R)$ are the following. (i) As the Z of the alkali-metal atom increases, the position of the maximum peak of the coupling shifts to larger R (peak position of $NaH^+ \simeq 11.5a_0$, $CsH^+ \simeq 17.5a_0$) and the position of the minimum of $\Delta E(R)$ also shifts in the same direction, (ii) the maximum position of the peak of the coupling does not match with the minimum position of ΔE (the maximum peak of the couplings lie at smaller-R values), (iii) KH^+ and RbH^+ share similar values of physical properties such as orbital radii, ionization potentials, and dipole polarizabilities; these

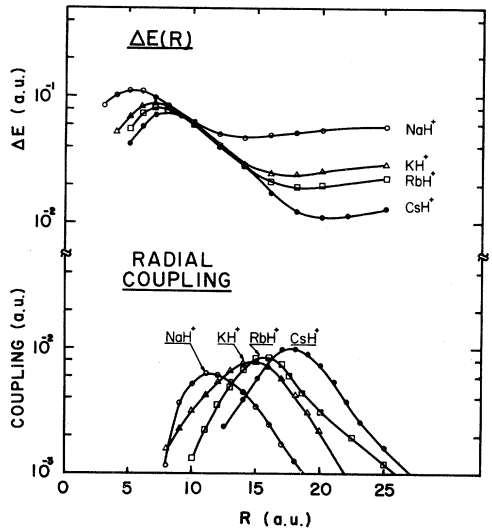

FIG. 6. Potential-energy differences between the $A\,^2\Sigma^+$ and $B\,^2\Sigma^+$ molecular states. Also shown are the long-range $A\,^2\Sigma^+ \rightarrow B\,^2\Sigma^+$ radial coupling matrix elements.

characteristics produce similar potential curves and couplings for both systems.

Some coupling matrix elements in the CsH^+ system have been reported by Olson *et al.*[2] along with the electron-capture cross sections (they did not include the ETF's correction). Our $A\,^2\Sigma^+ - B\,^2\Sigma^+$ radial coupling matrix element in CsH^+ is somewhat smaller in magnitude than that of Olson *et al.*, while the $A\,^2\Sigma^+$ to $C\,^2\Pi$ rotational couplings show similar structure. Turning to the NaH^+ system, the $A\,^2\Sigma^+ - B\,^2\Sigma^+$ and $A\,^2\Sigma^+ - C\,^2\Sigma^+$ radial couplings have been reported by Valance *et al.*[25] However, these authors have not published calculated cross sections. Their $A\,^2\Sigma^+ - B\,^2\Sigma^+$ radial coupling is about 15% larger in magnitude at the maximum when compared to ours. Unfortunately, Kubach and Sidis[6] have not published the coupling matrix elements used in their cross-section computations. Hence we are not able to compare our results to theirs.

B. Collision mechanisms

We have performed two-, three-, four-, six-, and eight-molecular-state coupled calculations for the $[H+M]^+$ systems. The dominant states involved are the near-resonant electron-capture states consisting of the $B\,^2\Sigma^+$, $C\,^2\Pi$, and $D\,^2\Sigma^+$ states [all correspond to the $H(n=2)$ manifold], in addition to the $A\,^2\Sigma^+$ $M(ns)$ ground state. The most important state which governs the electron-capture cross section is the $B\,^2\Sigma^+$ state which is strongly coupled to the $A\,^2\Sigma^+$ state by radial coupling at relatively large internuclear separations. A study of the two- and three-state calculation results shows that the contribution from the $B\,^2\Sigma^+$ state to the total charge transfer process is at least 60% in all cases. A major contribution is made also by the $C\,^2\Pi$ state which crosses the $B\,^2\Sigma^+$ state at relatively small-R values and approaches the $A\,^2\Sigma^+$ state at small R. We find strong rotational coupling between the initial $A\,^2\Sigma^+$ and final $C\,^2\Pi$ state for small impact-parameter collisions. Also, the $C\,^2\Pi$ state plays an important role as an intermediate state for flux promotion through strong angular coupling at the $B\,^2\Sigma^+ - C\,^2\Pi$ crossing region.

Our two-state ($A\,^2\Sigma^+, B\,^2\Sigma^+$) and three-state ($A\,^2\Sigma^+, B\,^2\Sigma^+, C\,^2\Pi$) calculations indicate that the dominant charge transfer processes in electron capture from ground-state alkali-metal atoms are $A\,^2\Sigma^+ \rightarrow B\,^2\Sigma^+$ radial coupling at large R, $A\,^2\Sigma^+ \rightarrow C\,^2\Pi$ rotational coupling at small R, and the two-step process $A\,^2\Sigma^+ \rightarrow C\,^2\Pi \rightarrow B\,^2\Sigma^+$ at intermediate R caused by rotational coupling between the $B\,^2\Sigma^+$ and $C\,^2\Pi$ states near the curve crossing. This picture is also confirmed by a collision-history study in which we observe the time dependence of the scattering process. The $D\,^2\Sigma^+$ state also couples with the $A\,^2\Sigma^+$ state strongly at small R, but it has a relatively large energy gap. The $D\,^2\Sigma^+$ plays an important part in redistributing the flux in the $H(n=2)$ manifold by long-range rotational and radial couplings on the outgoing part of the collision. Thus we conclude that a minimum of three ($B\,^2\Sigma^+, C\,^2\Pi, D\,^2\Sigma^+$) electron-capture states along with the initial $A\,^2\Sigma^+$ state should be included in the molecular expansion basis to obtain an accurate cross section for capture from ground-state alkali-metal atoms.

For electron capture by protons from excited alkali-metal atoms $H^+ + M^*(np)$, there are two molecular states which are asymptotically connected to the initial levels, $F\,^2\Sigma^+$ and $E\,^2\Pi$. The statistical weights for the particles following these molecular states are $\frac{1}{3}$ and $\frac{2}{3}$, respectively. We find strong radial coupling between the $F\,^2\Sigma^+$ and $D\,^2\Sigma^+$ states in the region $R \approx 18a_0$. However, the $E\,^2\Pi$ states do not couple strongly at large R with any of the electron-capture channels, either via radial or rotational coupling. Hence, approximately two thirds of the incident flux is lost to nonreaction. Correspondingly, the total electron-capture cross sections are much smaller than predicted using arguments based on the asymptotic energy gaps ΔE to the product channels.

The above behavior implies that the electron-capture cross section from $M^*(np)$ will be highly dependent on the polarization of the laser beam relative to the collision axis. If the $F\,^2\Sigma^+$ molecular state is pumped, the cross sections may be several orders of magnitude larger than if the $E\,^2\Pi$ molecular state is preferentially pumped, even at the same collision energy. Numerical results are given in the next section.

C. Cross sections

The calculated total electron capture and detailed cross sections for $H(2s)$ and $H(2p)$ formation for the $H^+ + M(ns)$ systems, with $M \equiv$ Na, K, Rb, and Cs, are shown in Figs. 7–10 and presented numerically in Table III. Similarly, results are also given for the $H^+ + M^*(np)$ collision systems. The calculations are directly compared to the recent experimental data of Nagata,[11] which are representative of the numerous measurements performed on the

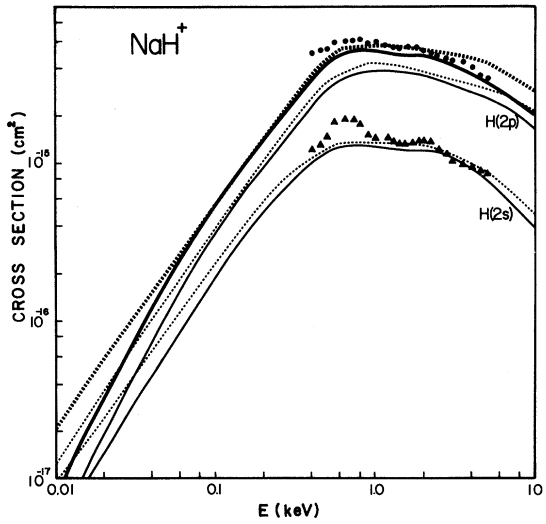

FIG. 7. Calculated electron-capture cross sections for $H^+ + Na(3s)$ collisions are denoted by solid lines and those for $H^+ + Na^*(3p)$ collisions by dashed lines. The heavy solid and dashed lines belong to the total capture cross sections. The detailed $H(2s)$ and $H(2p)$ cross sections are labeled. Experimental cross sections of Nagata (Ref. 11) are given by solid circles for total electron capture and by solid triangles for $H(2s)$ production for collisions of H^+ with ground state $Na(3s)$.

ground-state alkali-metal atom systems. A comprehensive review of available experimental data has been presented by Schlachter.[26]

The calculated results displayed in the figures employed an eight-state molecular expansion basis

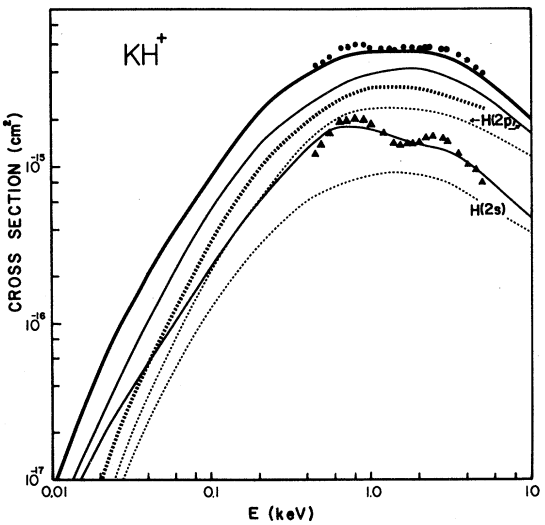

FIG. 8. Electron-capture cross sections for $H^+ + K(4s)$ and $H^+ + K^*(4p)$ collisions. The same notation is used as in Fig. 7.

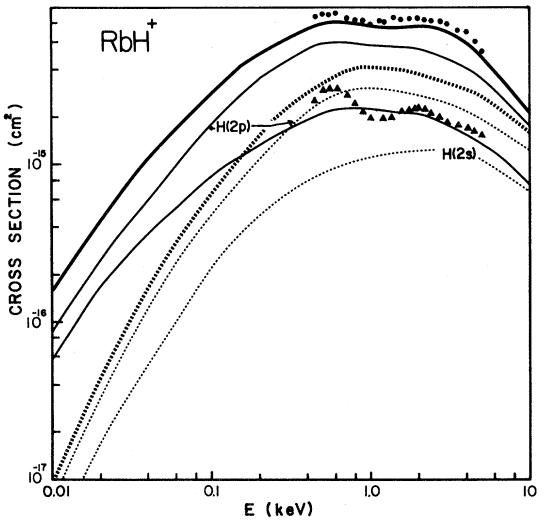

FIG. 9. Electron-capture cross sections for $H^+ + Rb(5s)$ and $H^+ + Rb^*(5p)$ collisions. The same notation is used as in Fig. 7.

set. These states included the $A\,^2\Sigma^+$ state arising from $H^+ + M(ns)$, the $B\,^2\Sigma^+$, $C\,^2\Pi$, and $D\,^2\Sigma^+$ states from $H(n=2) + M^+$, the $X\,^2\Sigma^+$ state from $H(1s) + M^+$, the $F\,^2\Sigma^+$ and $E\,^2\Pi$ states from $H^+ + M^*(np)$, and the $G\,^2\Sigma^+$ state from $H^+ + M^*[(n+1)s$ or $(n-1)d]$. To check the convergence of the cross section as a function of basis-set size, we included the next higher $^2\Sigma^+$ excited state in place of the $X\,^2\Sigma^+$ state which contributes a negligible amount to the cross sections.

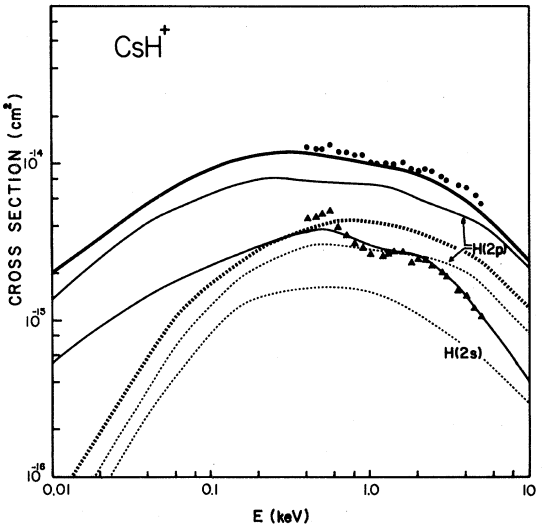

FIG. 10. Electron-capture cross sections for $H^+ + Cs(6s)$ and $H^+ + Cs^*(6p)$ collisions. The same notation is used as in Fig. 7.

TABLE III. Calculated total electron-capture cross sections (in units of 10^{-15} cm^2). (a) $H^+ + M(ns)$ collisions, (b) $H^+ + M^*(np)$ collisions; $M \equiv$ Na, K, Rb, and Cs.

E (keV)	NaH^+	KH^+	RbH^+	CsH^+
		(a)		
0.01	6.24×10^{-3}	7.89×10^{-2}	1.45×10^{-1}	2.03
0.05	1.82×10^{-1}	3.14×10^{-1}	1.34	6.81
0.1	5.61×10^{-1}	8.78×10^{-1}	2.71	9.13
0.5	4.20	4.40	8.04	11.2
1.0	5.13	5.42	7.71	10.2
5.0	3.48	3.69	4.77	4.97
10.0	1.98	1.99	2.18	2.37
		(b)		
0.01	2.09×10^{-2}	7.74×10^{-3}	2.22×10^{-2}	7.56×10^{-2}
0.05	2.08×10^{-1}	1.04×10^{-1}	2.84×10^{-1}	8.42×10^{-1}
0.1	6.41×10^{-1}	3.43×10^{-1}	7.81×10^{-1}	1.81
0.5	4.48	2.35	3.44	4.11
1.0	5.76	3.52	4.37	4.32
5.0	4.32	2.73	2.78	2.42
10.0	2.99	1.82	1.73	1.16

A classical-trajectory approximation was used for the heavy-particle motion. We have employed both straight-line trajectories and curvilinear trajectories to test the validity of the straight-line trajectory approximation. We found that the reduction of the cross sections due to the use of curvilinear trajectories is at most 10% at 0.1 keV in the light alkali-metal atom systems. The effect is less pronounced for the heavier alkali-metal atom systems, since the cross sections are primarily determined by long-range interactions. At energies $E > 0.1$ keV, the use of straight-line trajectories is valid. However, in the low-energy collision study ($E \leq 0.1$ keV), we found it necessary to employ curvilinear trajectories which were determined by the repulsive potential of the initial channel.

1. H^+—alkali-metal (ns) collisions

Our $H^+ + K$, $H^+ + Rb$, and $H^+ + Cs$ total charge transfer cross sections shown in Figs. 8—10 agree quite well with the recent measurements of Nagata[11] and also, with the recent theoretical results by Kubach and Sidis[6] (not shown). For the detailed H(2s) cross sections we reproduce the oscillatory structure observed experimentally, although with smaller amplitudes than indicated by the measurements. These oscillations are caused by a maximum in the difference of the potential energies between the $B\,^2\Sigma^+$ and the $D\,^2\Sigma^+$ states. This gives rise to nonrandom phase contributions to the cross sections. This interpretation is further confirmed by the fact that the H(2s) and H(2p) formation cross sections are out of phase with each other.

As a test of the convergence of the electron-capture cross sections in terms of the expansion basis set, we have carried out the cross-section calculations to channels other than the H($n=2$) electron-capture channels. The electron-capture cross sections to the H(1s) ground state for $H^+ + M(ns)$ collisions are at most approximately 0.1% of the total electron-capture cross section at 10 keV and are a negligible contribution to the total cross section at low energies. Numerical values for the H(1s) production cross sections are presented in Table IV and are probably accurate to only a factor of 2 or 3 because of their sensitivity to the description of the repulsive wall of the potentials where the pseudopotential method begins to fail.

TABLE IV. Detailed electron-capture cross section to the H(1s) ground state for $H^+ + M(ns)$ collisions (in units of 10^{-15} cm^2).

E (keV)	NaH^+	KH^+	RbH^+	CsH^+
0.1	2.21×10^{-5}	1.45×10^{-5}	1.21×10^{-5}	7.92×10^{-6}
1	3.26×10^{-4}	1.82×10^{-4}	1.28×10^{-4}	5.21×10^{-5}
10	1.38×10^{-3}	7.84×10^{-4}	5.42×10^{-4}	2.12×10^{-4}

The inclusion of the $H^+ + M^*$ excited states had a small effect on the magnitude of the electron-capture cross sections. Direct excitation cross sections to $H^+ + M^*$ products increased rapidly with increasing collision energy and attained values of $\sim 25\%$ of the total electron-capture cross sections at 10 keV. The mechanism of direct excitation to M^* excited states is most probably due to the two-step process with the $H(n=2) + M^+$ levels as intermediates. We have examined the convergence of the cross section as a function of expansion basis size at 0.1, 1, and 10 keV. Taking the CsH^+ system as a typical example, as we increase the basis from four-states to eight-states by adding the $X\,^2\Sigma^+$ and the Cs excited states, the electron-capture cross sections decrease by only 0.43%, 3%, and 9.7% at 0.1, 1, and 10 keV, respectively. Therefore, the electron transfer cross sections are reaching convergence in the energy region studied. As the energy is further increased above ~ 10 keV, ionization effects dominate so that the theoretical description which includes only bound states becomes invalid.

We next investigated the interesting case of H^+-Na($3s$) collisions (Fig. 7). Our calculated results are in very good agreement with the recent experimental data of Nagata,[11] but not with the older data by Grüebler *et al.*[7] The calculations of Kubach and Sidis[6] show a large disagreement with experiment in the low-energy region. Their calculated values are over an order of magnitude below the data at $E \leq 0.5$ keV. It is impossible for us to trace the origin of the discrepancies. However, as we have pointed out, Kubach and Sidis used an exceedingly small basis set to generate the eigenfunctions, which made it necessary to artificially shift the asymptotic limits of the molecular eigenenergies in order to perform the scattering calculations. Since the nonadiabatic coupling matrix elements are very sensitive to the shape of the wave functions, and because ETF effects were neglected, it is quite probable the calculations are in error. Direct comparison between the various experimental and theoretical results for NaH^+ have been presented elsewhere.[27]

2. $H^+ + M^*(np)$ collisions

Presented in Figs. 7—10 and in Table III are calculated cross sections for electron capture from the resonance state of the alkali-metal atoms [Eq. (2)]. The magnitude of these cross sections is similar to those for capture from the ground state for the lighter alkali-metal atoms, but it is smaller than the ground-state capture cross sections for the heavier alkali-metal atom systems.

These results can be understood by referring to the asymptotic energy gaps $\Delta E(\infty)$, to the electron-capture channels, and to the possible coupling mechanisms. Of importance is the fact that the $E\,^2\Pi$ state, which is asymptotically connected to the $H^+ + M^*(np)$ state, is not strongly coupled to the $H(n=2)$ electron-capture channels via either radial or rotational coupling. Hence the major entrance channel to the $H(n=2)$ manifold is the $F\,^2\Sigma^+$ state, which carries only one third of the incident flux. Thus even for the $H^+ + Na$ system where the $\Delta E(\infty)$ values for the major electron-capture states decrease from 1.74 eV for $H^+ + Na(3s)$ collisions to 0.36 eV for $H^+ + Na^*(3p)$ collisions, no significant enhancement in the cross section is predicted for collisions with excited $Na^*(3p)$. For the heavier alkali-metal atom systems the energy gap from the excited state to the electron-capture states becomes comparable to that from the ground state, so a decreased cross section is predicted and calculated.

Convergence tests for capture from $M^*(np)$ were examined as a function of basis-set size using the most difficult case $H^+ + Cs^*(6p)$. Calculations were performed using a small basis set which only included the three states from the $H(n=2)$ manifold and the two states from the initial $Cs^*(6p)$ level. These were compared to eight-state calculations which further included the $Cs^*(7s)$ level and two higher-lying states asymptotically connected to $Cs^*(5d)$. For energies $E \leq 1$ keV convergence was better than 10%, while at increased energies the importance of including higher-lying levels becomes important. At 10 keV, the results are converged to at least 26%, 29%, and 17% for the total electron capture and for the detailed $H(2s)$ and $H(2p)$ cross sections, respectively.

An interesting set of experiments has been reported by Kushawaha *et al.*[10] They have measured cross sections Lyman-α production, $H(2p) \rightarrow H(1s)$ transitions, and for collisions of H^+ with both ground Na($3s$) and excited $Na^*(3p)$ states at energies $E \leq 1$ keV. No difference in the cross sections was observed for energies from 0.02 to 1.0 keV. Our calculations (Fig. 7) confirm the measurements and show that enhancement due to collisions of $Na^*(3p)$ relative to Na($3s$) will only be important for $E < 20$ eV.

The calculations indicate that pronounced effects will be observed for electron capture from the resonance states of the alkali-metal atoms if specific

magnetic sublevels are populated by laser pumping. The use of a circularly or linearly polarized laser beam can preferentially populate either the $^2\Sigma^+$ or $^2\Pi$ sublevels of the $H^+ + M^*(np)$ manifold. Because the $^2\Pi$ state does not actively participate in the electron-capture process, one can expect large differences in the cross sections. Calculated cross-section ratios for initially producing either the $F\,^2\Sigma^+$ or $E\,^2\Pi$ state are presented in Table V. At collision energies $E \approx 0.1$ keV, differences of up to two orders of magnitude are predicted.

TABLE V. Ratio of cross sections for electron capture from the excited state $H^+ + M^*(np)$, where the entrance channel is prepared in the $F\,^2\Sigma^+$ and $E\,^2\Pi$ molecular states, respectively.

	Ratio $Q(F\,^2\Sigma^+)/Q(E\,^2\Pi)$			
E (keV)	NaH^+	KH^+	RbH^+	CsH^+
0.1	9.2	11	16	210
1.0	4.1	9.9	11	25
10.0	3.0	4.8	5.5	7.8

IV. CONCLUDING REMARKS

Pseudopotential molecular-structure calculations have been used to obtain information on the molecular structure of the LiH^+, NaH^+, KH^+, RbH^+, and CsH^+ systems. The wave functions were used to evaluate both radial and rotational coupling matrix elements for electron-capture cross-section calculations on all of these systems except LiH^+. In this latter case the near degeneracy between the $H^+ + Li^*(2p)$ and $H(n=2) + Li^+$ levels prohibited us from presenting accurate results.

The calculations employed electron translational factors which are necessary for the correct description of the asymptotic boundary conditions of the scattering equations. Spurious long-range couplings are thus eliminated and allow us, for the first time, to present accurate detailed cross sections for production of H(1s), H(2s), and H(2p). For capture from ground-state alkali-metal atoms our calculations are in good agreement with the measurements of Nagata.[11]

Of special interest are our studies on electron capture from the resonance state of the alkali-metal atoms $H^+ + M^*(np)$. Contrary to usual arguments we did not observe significant enhancement of the cross sections over those for capture from the ground state. This lies in our observation that the $E\,^2\Pi$ molecular state of the $H^+ + M^*(np)$ level does not participate actively in the electron-capture process. An interesting prediction is that the use of a polarized laser beam should show significant differences for capture from the $F\,^2\Sigma^+$ and $E\,^2\Pi$ states (see Table V).

ACKNOWLEDGMENTS

The authors would like to thank Dr. B. R. Junker for numerous helpful discussions and for providing us with the molecular-structure code. Travel funds for our collaboration was provided by North Atlantic Treaty Organization Grant No. RE.144.81. The research was supported by the Magnetic Fusion Energy division of the U. S. Department of Energy and by internal support from the Centre d' Etudes Nucléaires, Saclay.

[1] A. Valance and G. Spiess, J. Chem. Phys. 63, 1487 (1975).
[2] R. E. Olson, E. J. Shipsey, and J. C. Browne, Phys. Rev. A 13, 180 (1976).
[3] V. Sidis and C. Kubach, J. Phys. B 11, 2687 (1978).
[4] A. Valance, Chem. Phys. Lett. 56, 289 (1978).
[5] R. E. Olson, R. P. Saxon, and B. Liu, J. Phys. B 13, 297 (1980).
[6] C. Kubach and V. Sidis, Phys. Rev. A 23, 110 (1981).
[7] W. Grüebler, P. A. Schelzback, V. Kronig, and P. Marmier, Helv. Phys. Acta 43, 254 (1970).
[8] H. Scheidt, G. Spiess, A. Valance, and P. Pradel, J. Phys. B 11, 2665 (1978).
[9] C. J. Anderson, A. M. Howald, and L. W. Anderson, Nucl. Instrum. Methods 165, 583 (1979).
[10] V. S. Kushawaha, C. E. Burkhardt, and J. J. Leventhal, Phys. Rev. Lett. 45, 1686 (1980).
[11] T. Nagata, J. Phys. Soc. Jpn. 48, 2068 (1980).
[12] D. R. Bates, H. S. W. Massey, and A. L. Stewart, Proc. Phys. Soc. London, Sect. A 216, 437 (1953).
[13] M. Kimura and W. R. Thorson, Phys. Rev. A 24, 3014 (1981).
[14] T. A. Green, Phys. Rev. A 23, 532 (1981).
[15] G. J. Hatton, N. F. Lane, and T. G. Winter, J. Phys. B 12, L571 (1979); T. G. Winter and G. J. Hatton, Phys. Rev. A 21, 793 (1980).
[16] B. C. Garrett and D. G. Truhlar, in *Theoretical Chemistry: Advances and Perspectives,* edited by D. Henderson (Academic, New York, 1981), Vol. 6A, pp. 215–289.

[17]J. B. Delos, Rev. Mod. Phys. 53, 287 (1981).
[18]J. N. Bardsley, Case Stud. At. Phys. 4, 299 (1974).
[19]W. J. Stevens, A. M. Karo, and J. R. Hiskes, J. Chem. Phys. 74, 3989 (1981).
[20]R. E. Olson, R. P. Saxon, and B. Liu, J. Phys. B 13, 297 (1970).
[21]J. B. Delos and W. R. Thorson, J. Chem. Phys. 70, 1774 (1979).
[22]W. R. Thorson, M. Kimura, J. Choi, and S. K. Knudson, Phys. Rev. A 24, 1768 (1981).
[23]C. F. Melius and W. A. Goddard III, Phys. Rev. A 10, 1541 (1974).
[24]R. Bulirsch and J. Stoer, J. Numerische Mathematik. 8, 1 (1966).
[25]A. Valance, Q. Nguyen-Tuan, and K. Trinh Duc, *Abstracts of the XI ICPEAC, Kyoto, 1979,* edited by K. Takayanagi and N. Oda (The Society for Atomic Collisional Research, Kyoto, 1979), p. 516.
[26]A. S. Schlachter, in Proceedings of the Second International Symposium on Production and Neutralization of Negative H Ions and Beams, edited by T. Sluyters, Brookhaven National Laboratory Report No. BNL-51304 (unpublished), pp. 42—50.
[27]M. Kimura, R. E. Olson, and J. Pascale, Phys. Rev. A 26, 1138 (1982).